EIGHTEENTH
INTERNATIONAL
CONFERENCE ON
HYDRODYNAMICS
IN SHIP DESIGN, SAFETY
AND OPERATION

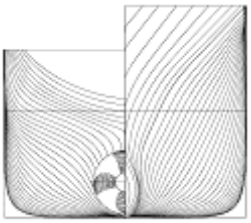

Verification of various methods for calculation of diffracted wave field around the ship

Paweł Wroniszewski[1], Jan Jankowski[1], Stefan Grochowalski[1]
[1] Polish Register of Shipping, Gdańsk, Poland

Diffracted waves around a simple, prolongated ship hull were calculated using source methods and boundary element method, for two and three dimensional models. The comparison of numerical results and experimental data is presented, together with the discussion of numerical and experimental methods.

Keywords: wave diffraction, Boundary Element Method

1 INTRODUCTION

Water trapped on deck of small vessel can cause capsizing of the vessel, therefore, proper evaluation of amount of water on deck is substantial. It depends on the actual position of the upper edge of bulwark and on the position of diffracted wave surface during the vessel motion in waves.

One of the essential elements of the water on deck problem is determination of actual deformed wave surface which is the result of superposition of velocity potential of incident wave and velocity potential of diffracted field. As the velocity potential of undisturbed wave is given in a form of a function, it is enough to solve the diffraction problem in order to determine the deformed wave elevation.

The paper presents four methods of solving the diffraction problem and validates them against a simplified shiplike body, for which appropriate experiments were carried out:

- Two and three dimensional wave source methods (2D WSM and 3D WSM);
- Two and three dimensional Rankine source methods (2D RSM and 3D RSM).

The results of computations for the experimental conditions by the four above methods are compared with the results of the experiments and discussed in the paper.

2 THE HYDRODYNAMIC BOUNDARY – VALUE PROBLEM DETERMINING THE DIFFRACTION

Neglecting viscous effects and assuming that water is incompressible and its flow irrotational, the diffraction problem can be formulated in terms of the potential flow theory. Assuming additionally, that incident waves of small amplitude are diffracted on the restrained body, the problem can be linearized. The assumption of linearity enables to superimpose the incident and diffracted wave fields to obtain the approximation of real waves around the restrained body.

The incident wave potential is given by the following formula:

$$\Phi_W(x,t) = i\zeta_A \frac{g}{\omega} e^{kx_3 - i\boldsymbol{k}\bar{x} - ik\delta + i(\omega t + \epsilon)} = \varphi_W(x) e^{i(\omega t+\epsilon)}, \quad x \in \mathbb{R}_3^- \tag{1}$$

where $\mathbb{R}_3^- = \{x : x_3 < 0\}$ is a lower half space, $x = (x_1, x_2, x_3)$, $\bar{x} = (x_1, x_2, 0)$, $\boldsymbol{k} = (k\cos\beta, k\sin\beta, 0) = (k_1, k_2, 0)$ is a wave vector, $k = \frac{\omega^2}{g}$ is the wave number, ω is the incident wave frequency, β is the angle between the wave vector and fixed vector in the body (normally, in the body symmetry plane, directed to the bow), and δ is the horizontal translation of the wave, in the direction of the wave vector.

The elevation of the water surface is determined by the formula:

$$\zeta_w(x,t) = -\frac{1}{g}\frac{\partial}{\partial t}\Phi(x,t)\Big|_{x_3=0} + \zeta_c, \tag{2}$$

where potential $\Phi = \Phi_W + \Phi_D$ is the sum of the potentials of the incident and diffracted wave, and ζ_c is the vertical translation of the wave. It is assumed, that the diffracted wave potential has similar form as wave potential:

$$\Phi_D(x,t) = \zeta_A \varphi(x) e^{i(\omega t+\epsilon)}, \tag{3}$$

where the time-independent part of the diffracted potential $\varphi(x)$ is determined by the following boundary-value problem (Jankowski, 2007):

- Laplace equation

$$\Delta\varphi(x) = 0 \quad x \in \mathbb{R}_3^- \backslash V, \tag{4}$$

where V is a closed domain occupied by the body, and the following boundary conditions:

- On the free surface:

$$\frac{\partial\varphi(x)}{\partial x_3} - k\varphi(x) = 0, \quad x \in S_F = \{x : x_3 = 0\} \backslash V \tag{5}$$

- On the wetted body:

$$\frac{\partial\varphi_D(x)}{\partial \boldsymbol{n}} = -\frac{\partial\varphi_W(x)}{\partial \boldsymbol{n}}, \quad x \in S_0 \tag{6}$$

  where φ_W is given by (1)

- At infinity:
  - radiation condition:

$$\lim_{\rho\to\infty} \sqrt{\rho}\left(\frac{\partial\varphi}{\partial\rho} + ik\varphi\right) = 0, \tag{7}$$

    where $\rho = \sqrt{(x_1 - y_1)^2 + (x_2 - y_2)^2}$;
  - condition at infinity on the free surface:

$$\lim_{\rho\to\infty} \sqrt{\rho}\,|\varphi| \leq c, \quad S_F = \{x : x_3 = 0\} \tag{8}$$

    where c is constant;
  - at the bottom:

$$\lim_{x_3\to-\infty} \frac{\partial\varphi}{\partial x_3} = 0. \tag{9}$$

The solution to the problem is not simple and requires application of an approximate method to determine the diffracted waves. Usually, the integral identities are used to solve the problem numerically, however, the fundamental solutions (or Green functions) must be given in explicit form.

3 FUNDAMENTAL SOLUTIONS OF THE BOUNDARY – VALUE PROBLEM

Depending on the method used to solve the problem (4) to (9) various fundamental solutions are used:

1. Fundamental solution in three dimensions (3D) satisfying Laplace equation, condition on the free surface and radiation condition and condition at infinity on the free surface (Jankowski, 2007):

$$E(x,y) = -\frac{1}{4\pi}\left[\frac{1}{|x-y|} - \frac{1}{|x-z|} + G(x,z)\right], \quad x,y \in \mathbb{R}_3^-, \quad x \neq y \tag{10}$$

where $x = (x_1, x_2, x_3)$, $y = (y_1, y_2, y_3)$ and $z = (y_1, y_2, -y_3)$

$$|x-y| = \sqrt{(x_1-y_1)^2 + (x_2-y_2)^2 + (x_3-y_3)^2} \tag{11}$$

$$|x-z| = \sqrt{(x_1-y_1)^2 + (x_2-y_2)^2 + (x_3+y_3)^2} \tag{12}$$

and G is harmonic function in the integral form (Jankowski, 2007):

$$G(x,y) = \frac{2}{|x-z|} - \frac{k}{\pi}\int_{-\pi}^{\pi} P.V.\,(J_1 + iJ_2)\,d\vartheta - ike^{k(x_3-z_3)}\int_{-\pi}^{\pi} e^{ik\chi}d\vartheta \tag{13}$$

where

$$\begin{aligned}
\chi &= (x_1-y_1)\cos\vartheta + (x_2-y_2)\sin\vartheta \\
P.V.J_1 &= e^{ky}\left[f\cos kx + g\sin kx\right], \\
P.V.J_2 &= e^{ky}\left[f\sin kx - g\cos kx\right], \\
f(r,\theta) &= \gamma + \ln(kr) + \sum_{n=1}^{\infty}\frac{(kr)^n\cos n\theta}{n!n}, \quad r \neq 0, \\
g(r,\theta) &= \theta + \sum_{n=1}^{\infty}\frac{(kr)^n\sin n\theta}{n!n}, \\
\theta &= \arctan\frac{\chi}{-(x_3-z_3)}
\end{aligned}$$

The first term of function (10) represents the Rankin source, the second – its symmetrical mirror reflection and the third – the pulsating source under free surface.

2. Fundamental solution in two dimensions (2D) satisfying Laplace equation, condition on the free surface and radiation condition and condition at infinity on the free surface (Jankowski &Wyrzykowski, 1992):

$$E(x,y) = -\frac{1}{2\pi}\left[\ln r + \ln r' - F(x,z)\right], \tag{14}$$

where $r = |\boldsymbol{x} - \boldsymbol{y}|$, $r' = |\boldsymbol{x} - \boldsymbol{z}|$, $x = (x_2, x_3)$, $y = (y_2, y_3)$, $z = (y_2, -y_3)$, and

$$\begin{aligned} F(x,z) &= F^R(x,z) + iF^I(x,z), \\ F^R(x,z) &= 2ke^{k\xi}\left[\cos(k\eta)\left(0.577215664 + \ln(kr_p) + C\right) + \sin(k\eta)\left(\theta + S\right)\right], \\ F^I(x,z) &= -2\pi ke^{k\xi}\cos(k\eta), \end{aligned} \tag{15}$$

where

$$\begin{aligned} \xi &= x_2 - y_2, \\ \eta &= x_3 + y_3, \\ r_p &= \sqrt{\xi^2 + \eta^2}, \\ \theta &= \arctan\left(-\frac{\eta}{\xi}\right), \\ C &= \sum_{n=1}^{\infty} \frac{f_n}{n}\cos(n\theta), \\ S &= \sum_{n=1}^{\infty} \frac{f_n}{n}\sin(n\theta), \\ f_n &= \frac{f_{n-1}}{n} r_p, \\ f_1 &= 1. \end{aligned}$$

3. Fundamental solution in 3D satisfying only Laplace equation (Marcinkowska, 1986):

$$E(x,y) = -\frac{1}{4\pi}\frac{1}{|x-y|}, \quad x, y \in \mathbb{R}_3^-, \quad x \neq y \tag{16}$$

where $x = (x_1, x_2, x_3)$, $y = (y_1, y_2, y_3)$. This is the first term of function (10) – the so called Rankine source.

4. Fundamental solution in 2D satisfying only Laplace equation (Marcinkowska, 1986)

$$E(x,y) = \frac{1}{2\pi}\ln|x-y|, \quad x, y \in \mathbb{R}_2^-, \quad x \neq y \tag{17}$$

where $x = (x_2, x_3)$, $y = (y_2, y_3)$. It is the Rankine source in 2D domain.

Thus the complexity of the fundamental solution depends on the number of boundary conditions the solution satisfies.

4 METHODS OF SOLVING THE HYDRODYNAMIC BOUNDARY – VALUE PROBLEM

In both methods presented below, the values of the potential in the computation domain are obtained by calculating the integrals over the boundary of the domain. The boundary is discretised, therefore the set of algebraic equations have to be solved. Such approach is in general called the Boundary Element Method.

Wave source method

In the case of using the fundamental solution (10) it is assumed that the solution to the boundary-value problem (4) to (9) takes the form of the following single layer potential:

$$\phi(x) = \int_{S_0} \mu(y) E(x,y) ds_y \tag{18}$$

where μ is the source density function (complex function of real variables), and S_0 is the wetted surface of the body (Fig. 1).

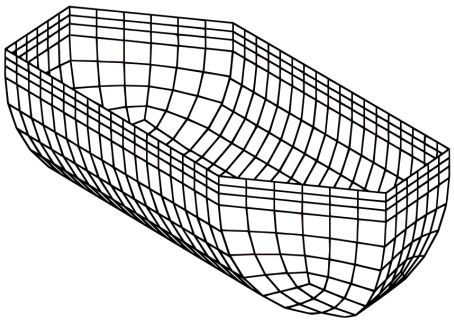

Figure 1: Wetted surface of the body

By substituting the singdile layer potential (18) to problem (4) to (9) the following Fredholm integral equation of second kind is obtained:

$$\frac{\mu(x)}{2} + \int_{S_0} \mu(y) \frac{\partial}{\partial_x \boldsymbol{n}} E(x,y)\, ds_y = \frac{\partial}{\partial_x \boldsymbol{n}} \varphi_W(x) \tag{19}$$

where $\boldsymbol{n}$ is the normal vector to S_0, directed to the water. The discretisation and solving the equation (19) is done according to (Jankowski, 2007).

The same approach is used to solve the problem using function (14), however, in this case the integral is over the cross section line of the cylindrical body (Fig. 2).

Rankine source method

In the case of using the fundamental solution in the form of (16) or (17) the following formula for harmonic functions, which represents the values in bounded domain by its

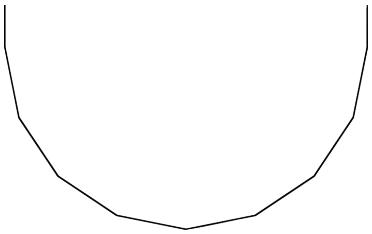

Figure 2: Cross section line

values and values of normal derivatives on the boundary – Fig. 3, (Marcinkowska, 1986), is used to solve the problem:

$$\varphi(x) = \int_{\partial\Omega} \varphi(y) \frac{\partial}{\partial_y \boldsymbol{n}} E(x,y)\ d\sigma_y - \int_{\partial\Omega} E(x,y)\ \frac{\partial}{\partial_y \boldsymbol{n}} \varphi(y)\ d\sigma_y; \tag{20}$$

normal vector is directed outside the domain. For 2D case the cross section of Ω is used to determine the diffraction potential.

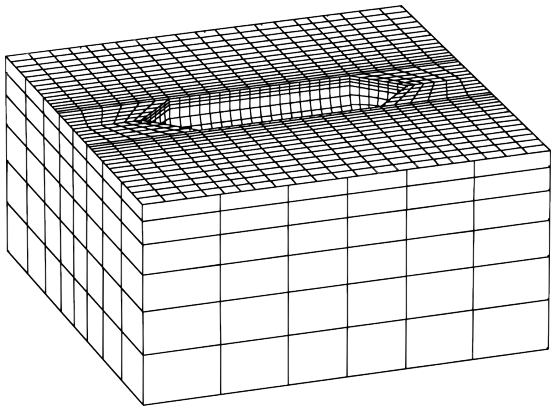

Figure 3: Bounded domain Ω in which diffraction potential is determined, using fundamental solution (16, 17)

Equation (20) determines the potential inside the domain Ω, unless the value of the potential and its derivatives on the boundary are known. Moving the point x into the boundary, the 'boundary-only' equation, that can be solve numerically, is obtained:

$$c(x)\varphi(x) = \int_{\partial\Omega} \varphi(y) \frac{\partial E(x,y)}{\partial_y \boldsymbol{n}}\ d\sigma_y - \int_{\partial\Omega} E(x,y)\ \frac{\partial \varphi(y)}{\partial_y \boldsymbol{n}}\ d\sigma_y. \tag{21}$$

The function $c(x)$ is caused by the singularity under the integrals (20), which appears when the point x is moved to the boundary. The singularity can be estimated by surrounding the boundary point x by a small sphere of radius ϵ, and calculating the integrals in equation (20) in the limit as $\epsilon \to 0$. It can be shown (Marcinkowska (1986)), that for a smooth boundary, for both 2D and 3D problems, the function $c(x)$ is constant and equal to 0.5.

To solve the equation (21) numerically, the boundary (surface) of the domain $\partial\Omega$ has to be discretised into N elements (panels) $\partial\Omega_i$, where $\sum_i^N \partial\Omega_i = \partial\Omega$ (Fig. 3) and the equation

can be written as a sum of integrals. Each element has a node at point x_i, located at the center of the element. Assuming that the value of the potential φ and its normal derivative is constant on each element and equal to the value in the node, they can be taken outside of the integrals. The set of equations for each element will consist of N equations of the form:

$$0.5\varphi_i - \sum_{j=1}^{N} \varphi_j \int_{\partial\Omega_j} \frac{\partial E\left(x_i, y\right)}{\partial_y \boldsymbol{n}} \; d\sigma_y = -\sum_{j=1}^{N} \frac{\partial \varphi_j}{\partial \boldsymbol{n}} \int_{\partial\Omega_j} E\left(x_i, y\right) \; d\sigma_y. \tag{22}$$

where the lower indices i, j indicate, that the value was taken in nodes x_i, x_j respectively. The following notation is used:

$$a_{ij} = -\int_{\partial\Omega_j} \frac{\partial E\left(x_i, y\right)}{\partial_y \boldsymbol{n}} \; d\sigma_y, \tag{23}$$

$$b_{ij} = -\int_{\partial\Omega_j} E\left(x_i, y\right) \; d\sigma_y. \tag{24}$$

If flat elements are used for the discretisation, all elements a_{ii} are equal to zero. Then the set of equations can be written in a matrix form:

$$A\varphi = B\frac{\partial \varphi}{\partial \boldsymbol{n}}, \tag{25}$$

$$\begin{bmatrix} 0.5 & a_{12} & \cdots & a_{1N} \\ a_{21} & 0.5 & \cdots & a_{2N} \\ \vdots & \vdots & \ddots & \vdots \\ a_{N1} & a_{N2} & \cdots & 0.5 \end{bmatrix} \begin{bmatrix} \varphi_1 \\ \varphi_2 \\ \vdots \\ \varphi_N \end{bmatrix} = \begin{bmatrix} b_{11} & b_{12} & \cdots & b_{1N} \\ b_{21} & b_{22} & \cdots & b_{2N} \\ \vdots & \vdots & \ddots & \vdots \\ b_{N1} & b_{N2} & \cdots & b_{NN} \end{bmatrix} \begin{bmatrix} \frac{\partial \varphi_1}{\partial \boldsymbol{n}} \\ \frac{\partial \varphi_2}{\partial \boldsymbol{n}} \\ \vdots \\ \frac{\partial \varphi_N}{\partial \boldsymbol{n}} \end{bmatrix}. \tag{26}$$

In fact, as the diffraction potential is a complex value, there are two sets of equations. To solve them, boundary conditions (5) to (9) are introduced, in order to specify either φ_i or $\frac{\partial \varphi_i}{\partial \boldsymbol{n}}$. The information provided by the boundary conditions can be in a form of a proper value given to the unknown (6), or as the relation between the potential and its derivative. The condition on the free surface (5) brings no difficulties, as it is identical with the normal derivation. As for the conditions at the infinity (7) to (9), it has been assumed that the borders of the computational domain are far enough from the ship hull to directly specify the conditions, saying that the direction $\boldsymbol{\rho}$ is identical with normal direction. It is assumed that the radiation condition (8) is automatically satisfied, what have been verified in the numerical results. The boundary conditions at the infinity (7) bring the relation between the real and imaginary parts, therefore actually one has to deal with an extended set of $2N$ equations, which can be solved using algebraic methods.

5 DESCRIPTION OF THE EXPERIMENT

The results of captive model tests dedicated to measurement of volume of water shipping on deck, carried out at the Institute for Marine Dynamics, Canada, are used for validation purpose in this work.

The tests in question were done in addition to experimental study of hydrodynamic forces generated on submerged part of deck in waves (Grochowalski, 1997). A cylindrical model with a constant cross-section in the form of semi-circle was used in the tests. The model was mounted rigidly to the tank carriage at various heading angles to oncoming waves and the tests were controlled and recorded on the carriage.

Oscillations of water level at the model sides were measured by one wave probe at each model side (Port and Starboard). In addition, the undisturbed waves were measured far from the model place (Xcal) and at the side of the model arrangement (Starboard Far). The experimental setup is shown in Fig. 4 and 5.

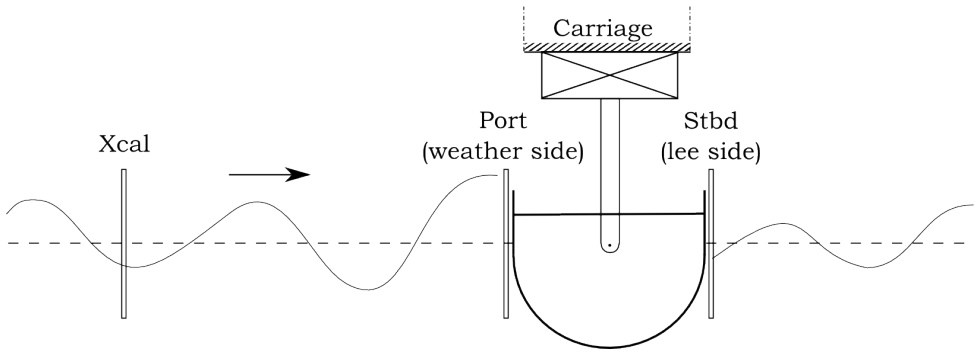

Figure 4: Experimental model

The test parameters were: model draft, wave height, wave length and profile, heading angle and model drift velocity. The undisturbed wave profile and the water oscillations at both model sides were recorded continuously at various combination of experiment parameters.

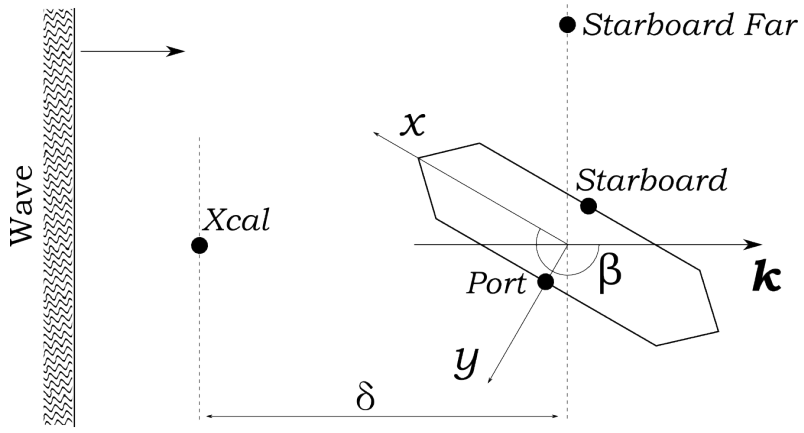

Figure 5: Experiment setup for model tests of water shipping on deck

An example of recorded data is presented in Fig. 6. These results together with the simple form of the model constitute an excellent basis for a validation of theoretical models representing wave diffraction and the numerical schemes for its computation.

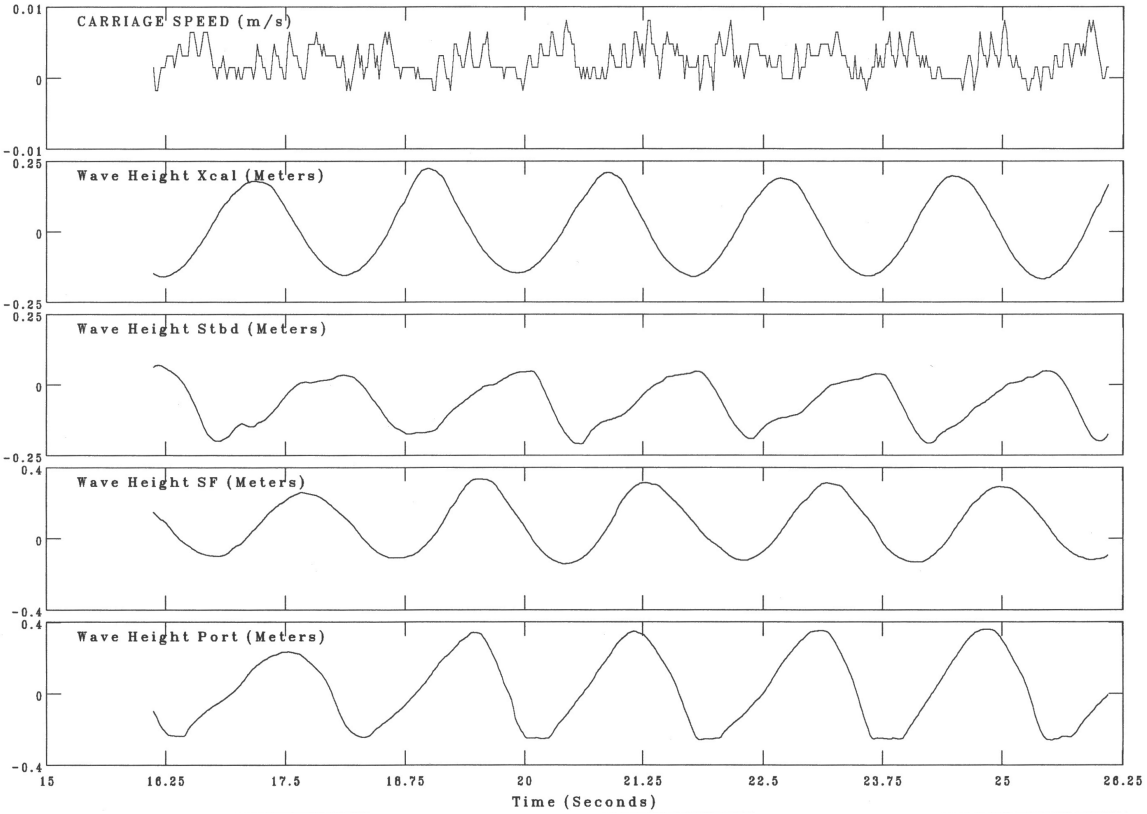

Figure 6: Example run from the experiment

6 COMPARISON OF THE COMPUTATION RESULTS WITH THE EXPERIMENTAL DATA

The numerical calculations were performed for the case of a beam wave, approaching the ship hull under the angle of 270^o (defined as in Fig. 5) and zero model drift velocity. Such case is easy to simplify from 3D to 2D, therefore the boundary element method and single layer potential method for both cases were used. Comparison of experimental data with computation results requires the proper incident wave potential, which has been obtained from the records of undisturbed wave (Xcal). The wave was separated into harmonics using discrete Fourier transform, and translated by the known distance δ (compare function (1)).

The comparison of the undisturbed wave recorded far before the model (Xcal) and the wave in the area close to the model (SF in Fig. 5) is presented in Fig. 7.

It should be taken into account that the undesirable influence of the walls of the towing tank could have taken place, as the water level measured by the probe on the side of the

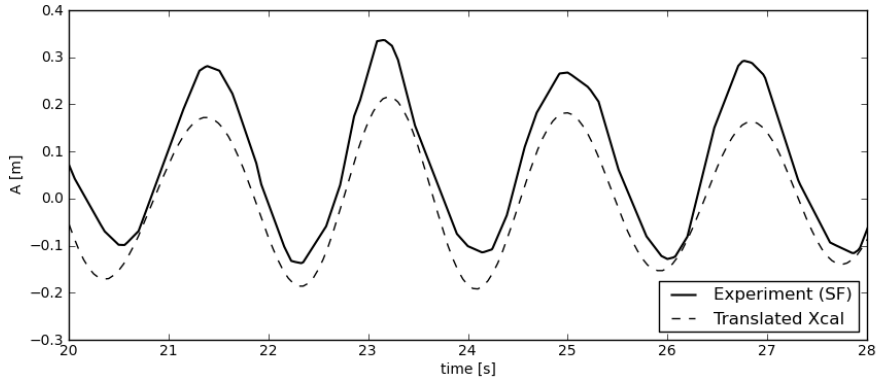

Figure 7: Example correlation between the translated Xcal wave used for calculations and the Starbord Far (SF) wave

model (SF probe) seems to be banked up. This effect seems to be not only due to the diffracted wave originating in the model.

The following graphs (Figures 8 to 11) present examples of comparison between numerical results and the experimental data.

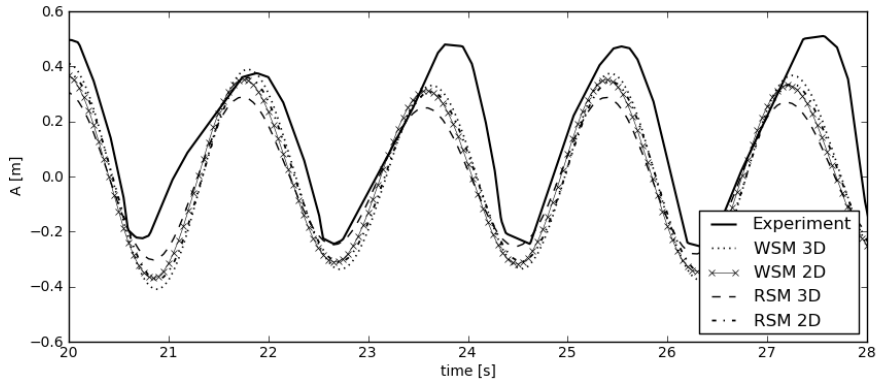

Figure 8: Experiment No. 38 - nominal wave period $T = 1.8$s, nominal amplitude $A = 0.19$m, model draft: $d = 0.1$m, Port (weather side)

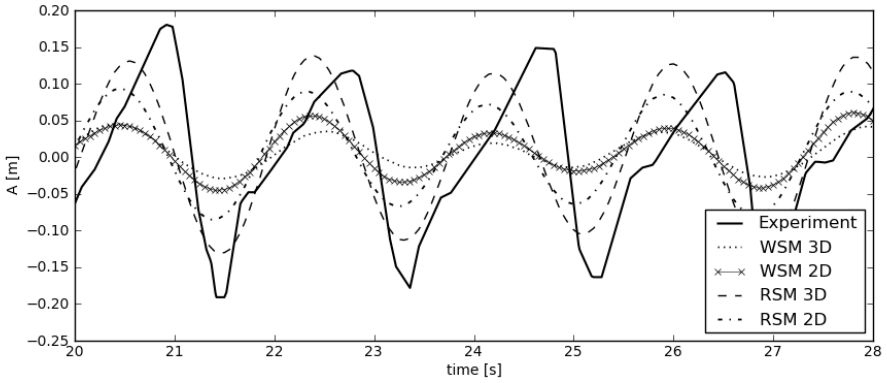

Figure 9: Experiment No. 38 - nominal wave period $T = 1.8$s, nominal amplitude $A = 0.19$m, model draft: $d = 0.1$m, Starboard (lee side)

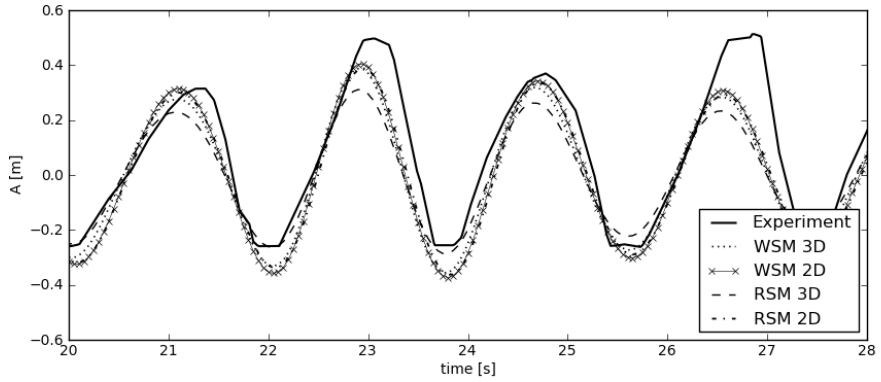

Figure 10: Experiment No. 41 - nominal wave period $T = 1.8$s, nominal amplitude $A = 0.19$m, model draft: $d = 0.04$m, Port (weather side)

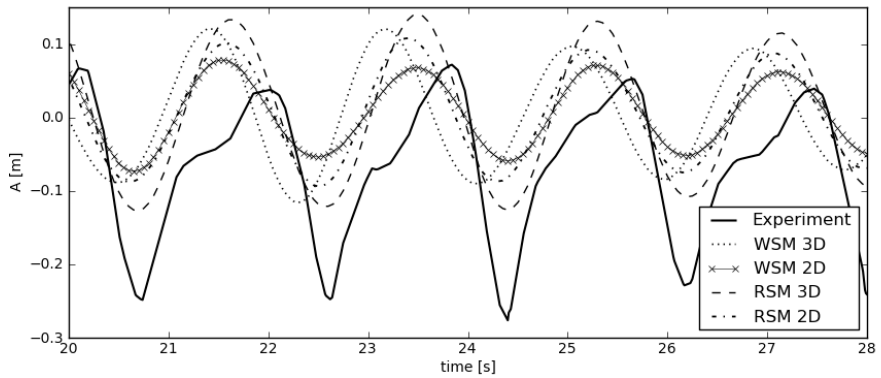

Figure 11: Experiment No. 41 - nominal wave period $T = 1.8$s, nominal amplitude $A = 0.19$m, model draft: $d = 0.04$m, Starboard (lee side)

There is essential eifference in the wave surface between the weather and the lee side. Large portion of the wave profile is damped by the presence of the body and the wave height at the lee side is significantly reduced. The theoretical methods reflect this difference to certain degree.

The theoretical methods presented here represent very well the deformation of waves at weather side, and all the methods give the results very close to each other. In case of the lee side, the theoretical methods differ between themselves and with the experimental results. The computation results which are the closest to the experiments are provided by the 3D Rankine source method (RSM 3D).

Although the correlation between the numerical calculation and the experiment data is not perfect, the better correlation is hardly to be expected by the linear, potential methods. The order of magnitude of the numerical results fits well into the experimental data for the weather side, while the nonlinearities could not be reflected well from the obvious reasons, in particular for the lee side.

7 CONCLUSIONS

The definition of the radiation conditions in the wave diffraction problem for use by the Rankine source method (RSM) is nontrivial, therefore one of the aims of this work was to verify if the approach provides relevant results. The results of the Rankine source method correlate well with the results of the wave source method (WSM) for the weather side. It means that the diffracted wave could freely leave the domain, without any reflection on the outer boundaries. The correlation on the lee side is not sufficient, and it requires further study.

Both methods have been proved usable. In the Rankine source method the system of algebraic equations that has to be solved is much bigger, as the equations are defined not only for the panels at the ship hull, but also for the mesh generated for the water surface, side-borders and lower-border of the computational domain. After calculations, the potential for each boundary element is given.

In case of the wave source method, the system of equations is smaller, but computation of the potential in each point requires more time, as complicated series have to be calculated. These features make the Rankine source method efficient for determination of whole diffracted wave field around the ship, while the wave source method seems to be better for computing the value of the potential in the required points in space.

The influence of the density of the computational mesh on the results should be studied, especially of the density of the free surface mesh in the Rankine source method.

The nonlinear effects seem to be significant in determining the free surface around the ship. Further studies of this topic should be continued.

REFERENCES

Grochowalski S., (1997), 'Experimental Investigation of the Hydrodynamic Forces and Pressure Distribution on the Submerged Part of Deck in Waves', Vol.1 Technical Report, National Research Council Canada, Institute for Marine Dynamics, TR-1997-09.

Jankowski J., (2007), 'Ship facing waves', Technical Report No. 52, Polish Register of Shipping, Gdańsk, Poland (in Polish).

Jankowski J., Wyrzykowski J., (1992), 'Continuation of Haskind's works', Transactions of the First Int. Conference in Commemoration of the Anniversary of Creating Russian Fleet by Peter the Great, St. Petersburg.

Marcinkowska H., (1986), Introduction to the partial differential equations, Wydawnictwo Naukowe PWN, Warsaw.

CONTACT DETAILS

Paweł Wroniszewski, Polish Register of Shipping, Hallera 126, 80-416 Gdańsk, Poland
pwroniszewski@prs.pl